ELSEVIER

Thermochimica Acta 334 (1999) 141–148

thermochimica acta

www.elsevier.com/locate/tca

Temperature programmed decomposition of cobalt ethylene diamine complexes

S. Dash*, P.K. Ajikumar, M. Kamruddin, A.K. Tyagi

Materials Science Division, Indira Gandhi Centre for Atomic Research, 603 102 Kalpakkam, India

Received 14 May 1998; accepted 10 June 1999

Abstract

The cobalt co-ordination complexes, $[Co(en)_2Cl_2]Cl$ and $[Co(en)_2CO_3]Cl$, synthesised through literature procedures, were characterised by FTIR. Trace metallic impurities were determined by ICP-MS. Crystallinity of the samples were ascertained by preliminary X-ray powder diffraction analysis. Dark field polarised optical microscopy (OM) was used to observe particle size distribution. These compounds were subjected to temperature programmed decomposition (TPD) in thermogravimetric analyser (TGA). TPD was also carried out in a home built mass spectrometry based evolved gas analyser (EGA-MS). The complex TGA weight loss profile could be successfully explained through EGA data. Complimentary information received from both the above techniques indicated sequential decomposition, prevalence of steric effect and functional group ejection. The non-isothermal kinetic analysis of TGA and EGA data showed dominance of kinetic control mechanisms based on sigmoidal rate laws like Avarami–Erofeev (AE) and random nucleation (RN). The fraction release $\alpha \sim T$ plots were used to evaluate integral model function $g(\alpha)$ of non-isothermal kinetic rate expressions. From $\log[g(\alpha)/T^2] \sim 1/T$ plots of well correlated model functions, Arrhenius parameters like activation energy and pre-exponential factors were evaluated for various decomposition steps.

Keywords: Co-ordination complex; Sequential decomposition; Steric effects; Activation energy

1. Introduction

Cobalt(III) ethylene diamine complexes constitute an important class of inorganic co-ordination compounds due to their fundamental as well as practical significance. Initial interest in $[Co(en)_2Cl_2]Cl$ accrued from optical isomerism [1]. Also this compound occurs as an important mechanistic intermediate in many inorganic preparations [2]. $[Co(en)_2CO_3]Cl$, a substituted derivative of the above compound is quite interesting from thermal decomposition and evolved gas studies angle. In this context, it is noteworthy that a large number of cobalt ethylene diamine complexes were investigated by Wendlandt et al. [3] using thermal analysis. However, complex weight loss behaviour during thermal decomposition, probably accruing from multistep sequential reactions was not explained [4]. In thermogravimetric analysis (TGA) and DTA investigation of $[Co(en)_2X_2]X$ type of halogen bearing compounds, Zsako et al. [5] had suggested that the complex weight loss behaviour is attributable to superposition of several intermediate reactions. In his paper, Ingier-stocka [6] had recommended dynamic thermal analysis as the best proce-

*Corresponding author.

0040-6031/99/$ – see front matter
PII: S0040-6031(99)00186-0

dure for comparison of thermal stability of homologous series of co-ordination complexes. In the light of the above, we have tried to explain the complex weight loss profiles of $[Co(en)_2Cl_2]Cl$ and $[Co(en)_2CO_3]Cl$ obtained from dynamic TGA runs through gaseous species data acquired from off-line dynamic EGA runs. Based on TGA and EGA-MS data, we have carried out comparison of thermal stabilities of these complexes. These data have also been used to derive the kinetics of various decomposition stages and obtain arrhenius parameters like activation energy and pre-exponential factor.

2. Preparation and characterisation

The cobalt ethylene diamine complexes were synthesised by wet chemical routes according to procedures outlined in literature [7]. The trans-dichloro-bis-ethylene diamine Co(III) chloride (hereafter known as compound I) was prepared by crystallisation from aqueous solution of $CoCl_2{\cdot}6H_2O$ and ethylene diamine. The compound II (carbonato-*bis*-ethylene diamine Co(III) chloride) was substitutionally derived from compound I by reaction with Na_2CO_3. The finely divided powder sample was observed by polarised optical microscopy in the dark field reflection mode [8]. The particles showed a size distribution over a narrow regime in the 15 ± 5 micron span [9]. Trace metallic constituents in these compounds were determined using an ELAN 250 Inductively coupled plasma mass spectrometer (ICP-MS) supplied by SCIEX, Canada [10]. The samples were dissolved in spectroscopically pure reagents and sprayed to ICP by use of a peristaltic pump and meinhard nebuliser [11]. Data were acquired by rapid scan mode. The instrument was calibrated using synthetic spectroscopically pure NBS traceable standards. Concentration of metallic impurities was found to be in micro-gm/gm level. These are presented in Table 1. The powder samples were blended with spectroscopic grade KBr powder and palletised. These pellets were subjected to FTIR analysis in the transmission mode. Vibrational assignments to FTIR spectra of these compounds acquired from a Perkin-Elmer spectrometer operating in the range 400–4500 cm^{-1} was carried out with the help of published literature [12]. Spectral matches were found within 2–3 wave numbers. Prominent infrared absorption bands for trans $[Co(en)_2Cl_2]Cl$ was assigned as following: for NH_2 the asymmetric deformation occurred at 1593 cm^{-1}, symmetric deformation at 1366 cm^{-1}, rocking mode at 806 cm^{-1}; for CH_2 the stretching mode was found at 2939 cm^{-1}, bending mode at 1464 cm^{-1}, wagging mode at 1272 cm^{-1} and twisting mode at 1115 cm^{-1} [13]. Unsplitting NH_2 asymmetric deformation frequency at 1593 cm^{-1} indicated *trans* character of the compound [14]. A similar observation has been reported for the isostructural compound $[Ir(en)_2Cl_2]Cl$ [15]. For its derivative compound, i.e. carbonato complex $[Co(en)_2CO_3]Cl$, following fundamental spectral absorption characteristics matches were noted [16]. CO_2 bending is observed at 758 cm^{-1}, CO_2 symmetric stretch at 1270 cm^{-1}, CO stretch at 1056 cm^{-1}, non-planar rocking at 832 cm^{-1} and asymmetric stretching at 1580 cm^{-1}. Barring external ion effect, the broad matching of data with spectral analysis of carbonato complex reveals prevalence of bidentate covalent nature of bonding [17]. Strong infrared absorption bands exhibited by ethylene diamene functional group [18,19] obscured the spectral characteristics of co-ordination compounds. These compounds were subjected to X-ray diffraction analysis in a Stoe powder diffraction system. The powders were found to be crystalline. $[Co(en)_2Cl_2]Cl$ showed a monoclinic crystal structure [20], whereas preliminary space group analysis suggested $[Co(en)_2CO_3]Cl$ to be triclinic.

Table 1
Trace metallic impurity analysis by ICP-MS

Sl. no.	Trace elements	Concentration (μg/g)	
		$[Co(en)_2Cl_2]Cl$	$[Co(en)_2CO_3]Cl$
1	Al	23	10
2	Ba	<5	<5
3	Cu	28	<5
4	Cr	<2	4
5	Fe	62	52
6	Mn	54	17
7	Mo	<2	<2
8	Ni	198	120
9	Pb	140	26
10	Sr	<5	<5
11	Ti	<2	<2
12	Zn	94	29

3. Experimental

TGA runs of these compounds were conducted in a Setram 92 TG, DTA apparatus using inert argon as flowing carrier gas at a heating rate of 10 K/m. Off-line mass spectrometry based evolved gas analysis (EGA-MS) studies were conducted under high vacuum conditions in our home built EGA-MS apparatus. Description of this facility is published elsewhere [21–23]. Essentially this facility is a high vacuum, high temperature resistance furnace coupled to an ultra high vacuum chamber housing a quadruple mass spectrometer through a leak valve. A computer assisted multiple ion detection, multichannel trend analysis mass spectrometry (MID-MS) software plots MID signals of evolved gases released from solids undergoing decomposition against specimen temperature to give EGA-MS plots.

4. Results and discussion

Compound I: Fig. 1 a shows the TGA plot of TPD of $[Co(en)_2Cl_2]Cl$. This complex profile is a convolution of several weight loss stages. Earlier works [24,25] have observed this behaviour for certain other amine based chloro compounds. In our studies the initial ~5% weight loss at 475 K was attributed to adsorbed moisture. This is substantiated by initial water release signal in EGA spectra, described below. Since our analysis was confined to thermal decomposition, this stage was not considered. Deconvolution of the TG profile showed four weight loss stages. These stages are marked in Fig. 1a as I, II, III and IV. The weight losses for these stages are 6.2%, 26.3%, 12.6% and 7.1% with temperature spans of 525–575, 570–725, 650–775 and 760–885 K respectively. The residue at 730 K corresponds to $CoCl_3$. The final weight loss is continuous. The above weight losses could be explained with the help of off-line EGA-MS studies. However, minor discrepancies

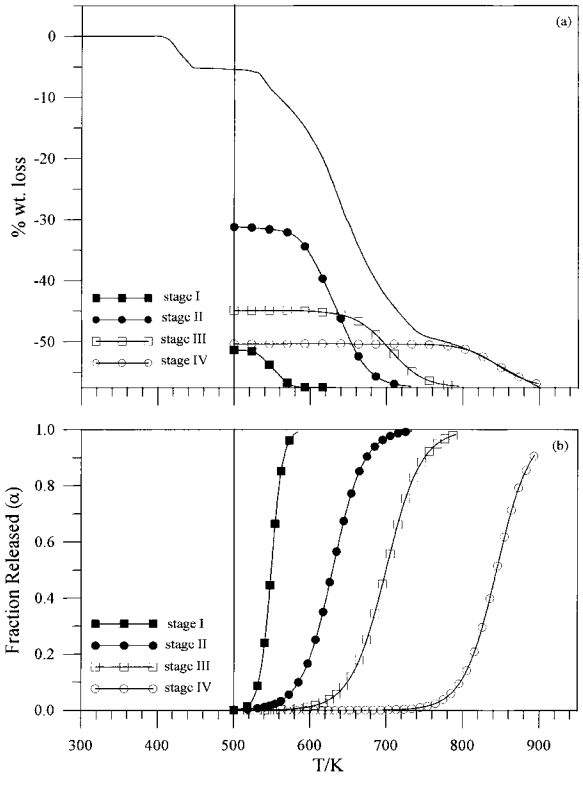

Fig. 1. (a) TGA plot with deconvoluted stages of TPD of $[Co(en)_2Cl_2]Cl$; (b) the corresponding fraction release plot.

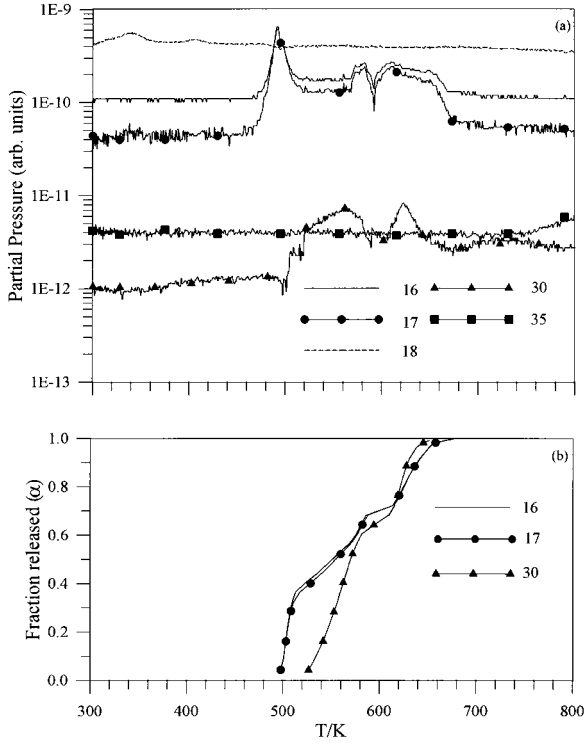

Fig. 2. (a) EGA-MS spectra of $[Co(en)_2Cl_2]Cl$; (b) the corresponding fraction release plot.

between these two studies are attributable to different sample environments.

The EGA-MS spectra of compound I is shown in Fig. 2a. The species corresponding to masses were: $m/e = 16$, CH_4; $m/e = 17$, NH_3; $m/e = 30$ and 43, ethylene diamine (en) fragments; $m/e = 35$, volatilised chlorine signals were detected. The decomposition occurs with concomitant release of CH_4 and NH_3. The CH_4 and NH_3 release is accompanied with en ejection. Formation of CH_4 and NH_3 can be attributed to bond cleavage effects. Also en fragmentation does not contribute to masses 16 and 17 [26]. As we have observed CH_4 and NH_3 species also, it suggests that out of the two en ligands one undergoes dissociation. The reason can be attributed to crystallographic inequivalence of en ligands in monoclinic unit cell of $[Co(en)_2Cl_2]Cl$ [27]. Based on these observations the weight loss steps can be ascribed to, stage I: NH_3 release; stage II: CH_4 and en ejection; stage III: release of remaining NH_3 and CH_4; stage IV: conversion of $CoCl_3 \rightarrow CoCl_2$. This is seen from detection of ^{35}Cl in EGA-MS beyond temperature 730 K.

In case of TPD of $[Co(en)_2Cl_2]Cl$, the EGA-MS spectra could successfully explain the TGA weight loss curve barring minor discrepancies. The discrepancies stem from different operating environments seen by the sample in TGA and EGA runs. In TGA runs NH_3 and CH_4 release occur in two stages and en ejection in single step. But in EGA-MS, the release of NH_3 and CH_4 occur in three overlapped stages and en in two stages. The temperature regimes were slightly lower. The reason for better resolution can be attributed to prevailing vacuum condition, which ensures near total irreversibility. The sequential multistep decomposition is in conformity with observation made in certain other Co(III) ethylene diamine based complexes. In these cases the internal co-ordination sphere ligands are sequentially replaced by external sphere anions [28]. Similar functional group ejection in other cobalt amine complexes had been reported by Zsako et al. [2]. They have also suggested substitution of internal sphere functional groups by external sphere anions as possible mechanisms.

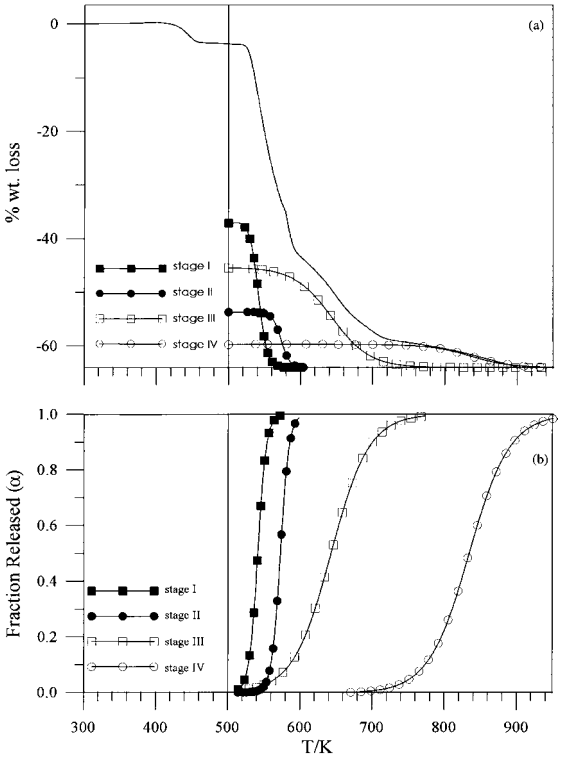

Fig. 3. (a) TGA plot with deconvoluted stages of TPD of $[Co(en)_2CO_3]Cl$; (b) the corresponding fraction release plot.

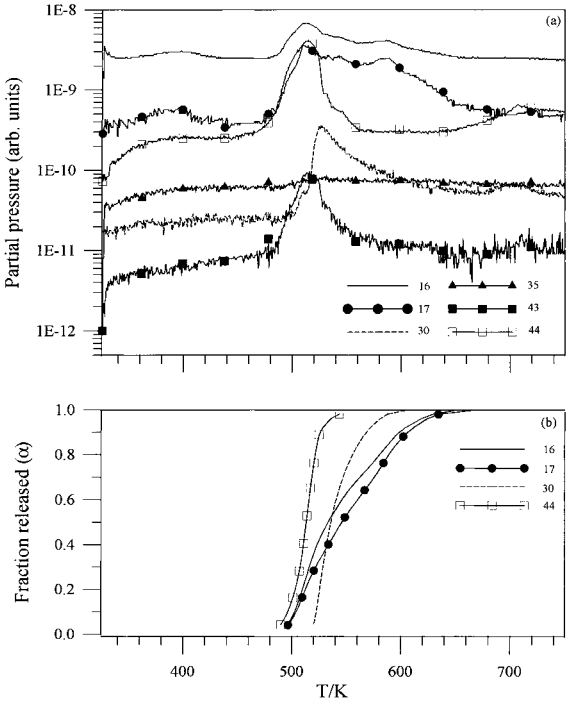

Fig. 4. (a) EGA-MS spectra of $[Co(en)_2CO_3]Cl$; (b) the corresponding fraction release plot.

Compound II: Deconvoluted TGA curve of TPD of $[Co(en)_2CO_3]Cl$ shows four weight loss stages (Fig. 3a). These weight losses are 27.2%, 10.3%, 18.6% and 4.3% at temperature spans of 525–565, 550–600, 600–700 and 700 K and above. Compared to compound I, various reaction initiation and completion temperatures in this compound are rather low. This can be attributed to steric instability arising from location of large carbonato oxyanion in the internal co-ordination sphere. Such steric instability has been reported for other amine based cobalt co-ordination compounds [29]. This instability is also responsible for various decomposition stages of compound II exhibiting smaller temperature spans than compound I. This compound yields $CoCl_2$ as final product at 730 K.

Here again, the weight losses are explainable on the basis of off-line EGA-MS runs. The EGA-MS spectra for this compound is given in Fig. 4. As seen from this figure, the gaseous products of decomposition are constituted by CH_4, NH_3, CO_2 and en indicating dissociation of one of the two en ligands. From the release profiles and temperature spans stage I weight loss can be attributed to release of $CH_4+NH_3+CO_2$, stage II is accounted by release of NH_3 and CH_4, en ejection explains stage III weight loss. Stage IV weight loss is due to continuous volatilisation of end product $CoCl_2$. Obviously the ^{35}Cl signature observed in the EGA-MS spectra of compound I is absent in this case. Volatilisation of reaction product $CoCl_2$ has also been reported by Wendlandt et al. [30] in their investigation of similar chloro amine compounds. The TGA weight loss stage match very well with EGA-MS data. The CO_2 release is single step and is concomitant with CH_4 and NH_3 release. CH_4 and NH_3 release extend beyond CO_2 and account for stage II weight loss. The TG data shows loss of en as stage III but in EGA en emission appears between two $CH_4 + NH_3$ release stages. This can be attributed to superior resolution of EGA over TGA especially where narrow temperature spans covering various reaction stages are encountered. Also the operating

Table 2
Non-isothermal, integral forms of kinetic expression for heterogeneous solid-state reactions

Reaction mechanism	Symbol	$f(\alpha)$	$g(\alpha) = \int_0^\infty d(\alpha)/f(\alpha)$
Nucleation and growth models			
Random nucleation approach			
(i) Mampel unimolecular law	A1	$1-\alpha$	$-\ln(1-\alpha)$
(ii) Avrami–Erofeev nuclei growth	A (1/*n*)	$1/n(1-\alpha)[-\ln(1-\alpha)]^{1-n}$	$[-\ln(1-\alpha)]^n$ $n = 1/4, 1/3, 1/2, 2/3$
(iii) Branching nuclei: (Prout–Tompkins)	B1	$\alpha(1-\alpha)$	$\ln[\alpha/(1-\alpha)]$
Accelerating rate equations			
(i) Power law	P (1/*n*)	$1/(n\alpha^{1-n})$	α^n $n = 1/4, 1/3, 1/2, 1, 3/2, 2$
(ii) Exponential law	En	$1/n\alpha$	$\ln \alpha^n$; $n = 1,2$
Decelerating rate equations			
(a) Based on diffusion mechanism			
(i) 1-dimensional diffusion	D1	α^{-1}	$\alpha^2/2$
(ii) 2-dimensional diffusion	D2	$[-\ln(1-\alpha)]^{-1}$	$(1-\alpha)[\ln(1-\alpha)]+\alpha$
(iii) 3-dimensional diffusion (Jander)	D3	$(1-\alpha)^{-1/3}[1-(1-\alpha)^{-1/3}]^{-1}$	$3/2[1-(1-\alpha)^{1/3}]^2$
(iv) 3-dimensional diffusion (Ginstling–Brounshtein)	D4	$[(1+\alpha)^{1/3}-1]^{-1}$	$3/2[1-2\alpha/3-(1-\alpha)^{2/3}]$
(v) 3-dimensional counter diffusion (Anti–Jander)	D5	$(1+\alpha)^{1/3}[1-(1+\alpha)^{-1/3}]^{-1}$	$3/2[(1+\alpha)^{1/3}-1]^2$
(b) Based on phase boundary movement			
(i) 1-dimensional (Zero order)	R1	Constant	α
(ii) 2-dimensional (cylindrical symmetry)	R2	$(1-\alpha)^{1/2}$	$2[1-(1-\alpha)^{1/2}]$
(iii) 3-dimensional (spherical symmetry)	R3	$(1-\alpha)^{2/3}$	$3[1-(1-\alpha)^{1/3}]$
(c) Based on order of reaction			
(i) Reaction order	Fn	$1/2(1-\alpha)^{1-n}$	$1-(1-\alpha)^n$; $n = 2,3,4$

environment at lower heating rate aids better resolution.

5. Kinetic analysis

Fraction release $\alpha_{(T)} \sim T$ curve were computed for TGA as well as EGA runs. These curves are shown in Fig. 1b and Fig. 3b for TGA runs and Fig. 2b and Fig. 4b for EGA runs. The integral model function $g(\alpha)$ for non-isothermal kinetic rate expressions were obtained and least square fitted to experimental values. Table 2 gives the non-isothermal kinetic rate expressions used by us [31,32]. The expression showing the best-correlated plot was considered to be the prevailing mechanism. From the slopes of $\ln[g(\alpha)/T^2] \sim 1/T$ plots, activation energies were deduced. The intercept of the plots yielded pre-exponential factor. Table 3 gives the details of prevailing mechanism, correlation coefficient, activation energy and pre-exponential factor for various weight loss and gas release stages.

The kinetic analysis of TGA and EGA results for various decomposition stages of these compounds

Table 3
Reaction mechanism, correlation coefficient, activation energy and pre-exponential factors obtained for various decomposition stages studied by TGA and EGA-MS techniques

Sample	Technique	m/z or species	Stage	α range	Reaction mechanism	E_A (KJ/mol)	Pre-exp. factor (m^{-1})	Correlation coefficient
$[Co(en)_2Cl_2]Cl$	TGA		I	0.18–78	AE($n = 3/2$)	160.436	8.8×10^{14}	0.99673
			II	0.2–78	RN	110.822	3.5×10^{8}	0.99788
			III	0.18–81	RN	119.335	1.6×10^{8}	0.99738
			IV	0.22–83	RN	206.219	1.5×10^{12}	0.99908
	EGA-MS	16	I	0.17–81	AE($n = 3/2$)	306.281	1.8×10^{31}	0.99569
			II	0.2–8	AE($n = 3/2$)	240.453	9.7×10^{20}	0.99746
			III	0.2–84	RN	220.271	2.1×10^{17}	0.98871
		17	I	0.21–8	AE($n = 3/2$)	294.913	1.2×10^{30}	0.99698
			II	0.17–81	RN	80.782	1.9×10^{6}	0.99736
			III	0.2–8	RN	231.603	1.9×10^{18}	0.98929
		en	I	0.2–8	RN	122.409	3.8×10^{10}	0.99971
			II	0.21–78	AE($n = 3/2$)	238.318	1.3×10^{19}	0.98362
$[Co(en)_2CO_3]Cl$	TGA		I	0.2–8	AE($n = 3/2$)	188.648	9.2×10^{17}	0.99704
			II	0.2–8	AE($n = 3/2$)	208.14	5.5×10^{18}	0.99712
			III	0.21–78	RN	84.287	1.1×10^{6}	0.99848
			IV	0.2–79	RN	135.74	4.9×10^{7}	0.99804
	EGA-MS	16	I	0.17–82	RN	202.916	9.8×10^{19}	0.99642
			II	0.18–82	RN	77.126	8.8×10^{5}	0.99749
		17	I	0.16–8	RN	186.992	1.9×10^{19}	0.99674
			II	0.16–81	RN	80.782	1.9×10^{6}	0.99736
		en	I	0.2–8	AE($n = 3/2$)	180.862	3.6×10^{17}	0.99418
		CO_2	I	0.21–81	RN	231.394	7.7×10^{22}	0.99937

reveal preponderance of sigmoidal character. Initial stages confirm to kinetic control by Avarami–Erofeev (AE) rate expressions having dimensionality 3/2. This dimensionality indicates complex but geometrically isotropic growth of product nuclei [33]. Such rapid nucleation process is indicative of many other solid state decomposition reactions where physical processes like structural phase transformations and recrystallation are encountered.

FTIR studies on transition metal ethylene diamene complexes have indicated evidence of strong hydrogen bonding [34] These hydrogen bonded structures are likely to undergo amorphosization due to hydrogen bond loss. Such solid state structural collapse leads to generation of nascent nucleation sites for predominantly surface desorption controlled random nucleation (RN) mechanism to proceed. This mechanism is expressed through Mampel unimolecular rate law. The intermediate kinetics observed by us indicates governance by RN approach. Such observations regarding prevalence of RN mechanism succeeding structural collapse have been observed by us in the TPD study of other H-bonded solids like Al-alum [35].

6. Conclusion

Cobalt ethylene diamene complexes, synthesised through literature procedures, were characterised by OM, FTIR and ICP-MS. Complimentary real time TGA and EGA-MS runs on TPD of the chloro-complex and its subtitutional carbonato derivative revealed sequential multistep decomposition. Owing to steric instability, the carbonato derivative had lower reaction initiation temperature as well as narrow temperature span for various decomposition stages. Important observations made by us like functional group ejection, $CoCl_2$ formation and end product volatilisation are consistent with reported literature giving TGA results on similar chloro amine complexes. The governance of sigmoidal rate laws like AE and RN expressions indicate persistence of active surfaces owing continued generation to bond disruptive effects. However, in this study, structural correlations addressing these effects have not been done. Hence, we plan to undertake high temperature real time X-ray diffraction measurements to map out structural transformation in condensed phase concomitant with observed gas release/decomposition stages.

Acknowledgements

The authors are grateful to Dr. Baldev Raj and Dr. T.S. Radhakrishnan for their constant and continued support. We also acknowledge the instrumentation support rendered by Dr. B. Purnaih and Shri J. Jayapandian. We are grateful to Dr. T.R. Mahalingam and Shri R. Krishna Prabhu for ICP-MS runs, Shri K. Varatharajan for optical microscopy and Dr. K.S. Viswanathan for useful discussion on FTIR data.

References

[1] R.D. Archer, in: S. Kirschner (Ed.), Co-ordination Chemistry, Plenum Press, New York, 1969.
[2] J. Zsako, M. Varhelyi, C.S. Varhelyi, J. Thermal Anal. 17 (1979) 123.
[3] W.W. Wendlandt, J.P. Smith, The Thermal Properties of Transition Metal Ammine Complexes, Elsevier, Amsterdam, 1967.
[4] W.W. Wendlandt, T.D. George, K.V. Krishnamurty, J. Inorg. Nucl. Chem. 21 (1961) 69.
[5] J. Zsako, M. Varhelyi, C.S. Varhelyi, Gy. Liptay, Thermochim. Acta 51 (1981) 277.
[6] E. Ingier-stocka, Thermochim. Acta 170 (1990) 107.
[7] J.B. Bailar, Inorganic Syntheses, McGraw-Hill, New York, vol. 2, 1946, p. 221.
[8] H.E. Knechtel, W.F. Kindle, J.L. McCall, R.D. Buchheit, in: T. Lyman (Ed.), Metals Handbook, vol. 8, American Society for Metals, OH, 1973, p. 10.
[9] D.A. Elkington, R. Wilson, in: P.J. Lloyd (Ed.), Particle Size Analysis, Wiley, New York, 1987, p. 261.
[10] T.R. Mahalingam, in: S.K. Aggarwal, H.C. Jain (Ed.), Introduction to Mass Spectrometry, Indian Society for Mass Spectrometry, 1997, p. 13.
[11] S. Vijaylakshmi, R. Krishna Prabhu, T.R. Mahalingam, C.K. Mathews, At. Spectrosc. 13(2) (1992) 61.
[12] K. Nakamoto, Infrared and Raman Spectra of Inorganic and Co-ordination Compounds, Wiley, New York, 1963, p. 208.
[13] M.L. Morris, D.H. Busch, J. Am. Chem. Soc. 82(7) (1960) 1521.
[14] T.A. McLean Jr., A.F. Schneifner, A.F. Laethem, J. Inorg. Nucl. Chem. 26 (1964) 1245.
[15] S. Kida, Bull. Chem. Soc. Japan 39 (1966) 2415.
[16] B.M. Gatehouse, S.E. Livingstone, R.S. Nyholn, J. Chem. Soc. part III, art. 636, 1958, p. 3137.
[17] J. Fujita, A.E. Martell, K. Nakamoto, J. Chem. Phys. 36(2) (1962) 339.
[18] D.B. Powel, Spectrochim. Acta 16 (1960) 241.

[19] B. Schrader, in: W. Meir (Ed.), DMS Raman/IR Atlas of Organic Compounds, vol. 1, Verlag Chemie, Weinheim, 1978, pp. A7–O7.
[20] J.M. Williams, Inorg. Nucl. Chem. Lett. 3 (1967) 297.
[21] M. Kamruddin, P.K. Ajikumar, S. Dash, B. Purniah, A.K. Tyagi, K. Krishan, Instr. Sci. Technol. 23(2) (1995) 123.
[22] M. Kamruddin, P.K. Ajikumar, S. Dash, R. Krishnan, A.K. Tyagi, K. Krishan, J. Thermal Anal. 48 (1997) 277.
[23] S. Dash, M. Kamruddin, A.K. Tyagi, Bull. Mater. Sci. 20(3) (1997) 359.
[24] J. Zsako, J. Horak, C.S. Varhelyi, J. Thermal Anal. 20 (1981) 435.
[25] R. Wojciechowska, P. Bragiel, M. Czerwinki, J. Thermal Anal. 36 (1990) 1295.
[26] A. Cornu, R. Massot, Compilation of Mass Spectral Data, Part A, Commisariat A L' Energie Atomique, vol. 1, Heyden and sons, London, 1975, p. 5A.
[27] R.W.G. Wyckoff, Crystal Structures, vol. 5, 2nd ed., InterScience Publishers, New York, 1996, p. 355.
[28] G. Grassini-Strazza, A. Cristalli, V. Carunchio, A. Messina, Thermochim. Acta 36 (1980) 161.
[29] R. Bucci, A.D. Magri, A.C. Magri, A. Messina, Thermochim. Acta 60 (1983) 287.
[30] W.W. Wendlandt, E.L. Simons, Thermochim. Acta 36 (1980) 239.
[31] A.B. Phadnis, V.V. Deshpande, Thermochim. Acta 62 (1983) 361.
[32] M.E. Brown, Introduction to Thermal Analysis, Chapman and Hall, London, 1988, p. 131.
[33] A.K. Galway, Chemistry of Solids, Science Paperbacks, Chapman and Hall, London, 1967, p. 173.
[34] D.B. Powel, N. Sheppard, Spectrochim. Acta 17 (1961) 68.
[35] M. Kamruddin, P.K. Ajikumar, S. Dash, R. Krishnan, A.K. Tyagi, K. Krishan, Thermochim. Acta 287 (1996) 13.